

<http://dx.doi.org/10.1016/j.polymdegradstab.2013.09.013>

# The effect of gas phase flame retardants on fire effluent toxicity

---

Shirley Molyneux, Anna A Stec, T Richard Hull,

Centre for Fire and Hazards Science, University of Central Lancashire, Preston, PR1 2HE, UK

## *Abstract*

Standard industry formulations of flame retarded aliphatic polyamides, meeting UL 94 V-0, have been burned under controlled conditions, and the yields of the major asphyxiants, carbon monoxide (CO) and hydrogen cyanide (HCN) have been quantified. Although both the combination of aluminium phosphinate and melamine polyphosphate, and the combination of brominated polystyrene and antimony oxide, inhibit combustion reactions in the gas phase, this study shows that the phosphorus causes a much smaller increase in the CO and HCN yields than antimony-bromine. The mechanisms of CO and HCN generation and destruction are related to the flame inhibition reactions. Both CO and HCN form early in the flame, and the OH radical is critical for their destruction. Crucial, in the context of the flame inhibition mechanism, is the observation that the phosphorus system reduces the H and O radical concentrations without a corresponding decrease in the OH radical concentration; conversely, the bromine system reduces all three of the key radical concentrations, H, O and OH, and thus increases the fire toxicity, by inhibiting decomposition of CO and HCN. Moreover, while the phosphorus flame retardant is effective as an ignition suppressant at lower temperatures (corresponding to early flaming), this effect “switches off” at high temperatures, minimising the potential increase in fire toxicity, once the fire develops. Since flame retardants are most effective as ignition suppressants, and at the early stages of flaming combustion, while most fire deaths and injuries result from toxic gas inhalation from more developed fires, it is clearly advantageous to have an effective gas phase flame retardant which only causes a small increase in the toxic product yields.

## *Keywords*

Polyamide, brominated, phosphinated, flame, retardant, toxic.

# 1 Introduction

## 1.1 Fire Hazards

UK fire statistics [1] show that the main cause of death in fires, and the main cause of injury, arises from the inhalation of toxic effluents. To assess the contribution of a material, or a composite article (such as a chair or a fuse box) to the fire toxicity, it is necessary to know both the rate of fire growth and the yields of the different toxicants. The composition of these effluents depends on the chemical formulation of the burning material, oxygen supply, temperature and heating rate [2,3]. The most toxicologically significant products are asphyxiant gases and incapacitating irritants. The asphyxiants, carbon monoxide (CO) and hydrogen cyanide (HCN), decrease the oxygen supply to body tissue resulting in central-nervous-system depression, loss of consciousness and ultimately death. Irritant gases, such as acid gases, hydrogen chloride (HCl) and hydrogen bromide (HBr), certain hydrocarbons and their oxygenated decomposition products, cause immediate incapacitation, mainly by their effects on the eyes and upper respiratory tract, followed by longer term damage deeper in the lung [4].

Certain fire retardants inhibit the free radical reactions typical of flaming combustion. These gas phase “*flame* retardants” have been shown to increase the yield of carbon monoxide and hydrogen cyanide, both products of incomplete combustion [5, 6].

Fires can be divided into a number of stages from smouldering combustion and early well-ventilated flaming, through to fully developed under-ventilated flaming (Table 1) [7]. A useful concept in characterising the gas phase flaming combustion conditions, and predicting the yields of products such as carbon monoxide (CO), carbon dioxide (CO<sub>2</sub>), hydrogen cyanide (HCN) and hydrocarbons, is the equivalence ratio ( $\phi$ ), presented in Equation 1 [8].

**Table 1 Stages of a fire (adapted from ISO classification)[7]**

Fire Stage	Max Temp /°C		Typical values	
	Fuel	Smoke	Equivalence ratio	CO/CO <sub>2</sub> ratio
			$\phi$	
<b>Non-flaming</b>				
1a. Self-sustained oxidative pyrolysis (e.g. smouldering)	450-800	25 - 85	-	0.1-1
<b>Well ventilated flaming</b>				
2. Well ventilated flaming	350-650	50 - 500	0.5 – 0.7	< 0.05
<b>Under ventilated Flaming</b>				
3a. Low ventilation room fire	300-600	50-500	1.5 – 2	0.2-0.4
3b. Post flashover	350-650	>600	1.5 – 2	0.1-0.4

$$\phi = \frac{\text{actual fuel to air ratio}}{\text{stoichiometric fuel to air ratio}}$$

$\phi = 1$       "stoichiometric" combustion  
 $\phi \ll 1$       well – ventilated fires (fuel lean flames)  
 $\phi > 1$       under – ventilated fires (fuel rich flames)

### Equation 1

When assessing fire toxicity, the toxic product yields show the greatest sensitivity to the combustion conditions. It is important to ensure that these are relevant to the full-scale fire scenario. It is therefore essential to the assessment of toxic hazard from fire that each fire stage can be adequately replicated, and preferably separating the individual fire stages. A number of different methods exist to assess fire toxicity [9], but most fail to relate the toxicity or toxic product yields to particular fire scenarios, or to replicate the most toxic under-ventilated conditions [3]. The steady state tube furnace (SSTF), ISO/DIS 19700 [10], was specifically designed to replicate individual fire stages. It is a bench scale tube furnace through which an 800 mm length of sample is driven at a fixed rate, inside a quartz boat. It is supplied with a fixed flow of primary air and the equivalence ratio,  $\phi$ , can be controlled, in order to replicate different ventilation conditions. The heat fluxes in the SSTF have been reported [11]: at a furnace temperature of 650 °C the heat flux was 40 kW m<sup>-2</sup>; at a furnace temperature of 825 °C the heat flux was 77 kW m<sup>-2</sup>.

## 1.2 Fire Toxicity

The contribution of individual toxicants to the overall toxicity can be expressed as a fractional effective dose (FED), described in an additive model of toxicity, as shown in Equation 2, based on rat lethality data to predict the toxicity of a fire effluent, ISO 13344 [12]. The concentration of each toxicant, X, is represented by [X] and each term is divided by the lethal concentration of that toxicant (LC<sub>50, X</sub>); the individual contributions are summed to give the overall toxicity, described as the fractional effective dose (FED). When the sum exceeds 1.0, the effluent would be lethal to 50% of the exposed population. A more sophisticated approach recognises that incapacitation, rather than actual death, is the critical event in terms of fire safety. This has been defined in ISO 13571 [13] using consensus estimates of human response to toxicants. The measurements from the SSTF are suited to both approaches, but only the simpler rat lethality model is used here. Experimental toxic product yields can be normalised to a fixed mass/volume loading. In this work, a fuel mass-charge concentration of 20 g m<sup>-3</sup> is used. This is equivalent to a fuel mass of 1 kg in a 50 m<sup>3</sup> room.

$$\text{FED} = \left\{ \frac{[\text{CO}]}{\text{LC}_{50,\text{CO}}} + \frac{[\text{HCN}]}{\text{LC}_{50,\text{HCN}}} + \frac{[\text{HCl}]}{\text{LC}_{50,\text{HCl}}} + \frac{[\text{NO}_2]}{\text{LC}_{50,\text{NO}_2}} + \dots + \text{organics} \right\} \times V_{\text{CO}_2} + A + \frac{21 - [\text{O}_2]}{21 - 5.4}$$

$$V_{\text{CO}_2} = 1 + \frac{\exp(0.14[\text{CO}_2]) - 1}{2}$$

A is an acidosis factor equal to  $[\text{CO}_2] \times 0.05$ .

### Equation 2

## 1.3 Toxic product yields of polyamide 6.6

Previous reports [3, 14] of the fire toxicity of polyamide 6 have shown that combustion is efficient at low equivalence ratios with low yields of CO, HCN and organics, all of which increase as the equivalence ratio exceeds 1. The yields for CO and HCN increase with decrease in ventilation, or

increase in  $\phi$ . In well-ventilated combustion conditions the CO yield was low, but increased steeply to a maximum of 0.32 g/g at  $\phi=2.3$ . The yield of HCN, another product of incomplete combustion, also increases with increasing  $\phi$ . The individual toxicant yields are shown in Figure 1, as a function of equivalence ratio.

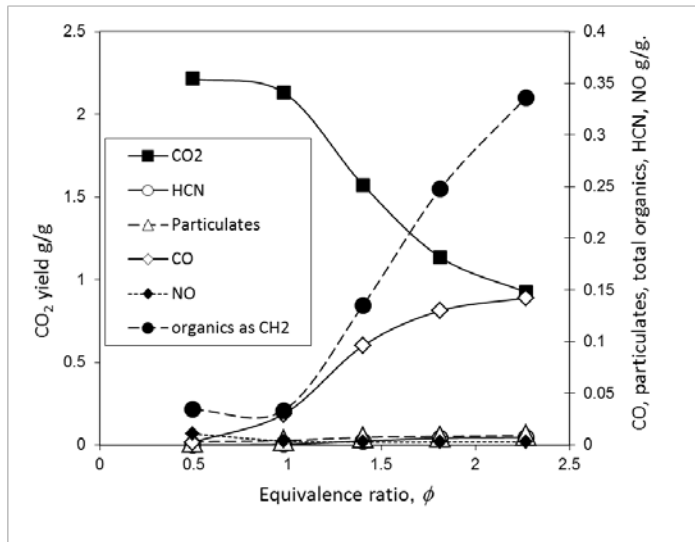


**Figure 1** Yields of toxicants from burning polyamide 6, over the temperature range 650-825 °C

Equation 2 can be applied to toxic product yields, such as those shown in Figure 1, in order to predict the toxicity of the effluent. This shows that for polyamide 6, the effluent toxicity and particularly the contribution of HCN grows significantly with under-ventilation, and increasing severity of fire. FED values of 6 or 8 may be interpreted as a polymer loading of 167 g or 125 g, respectively, burning in a 50 m<sup>3</sup> room, under the specified conditions, will be lethal to 50 % of the occupying population in 30 minutes exposure. The contribution of each toxic species to the FED has been calculated, and is presented in Figure 2.

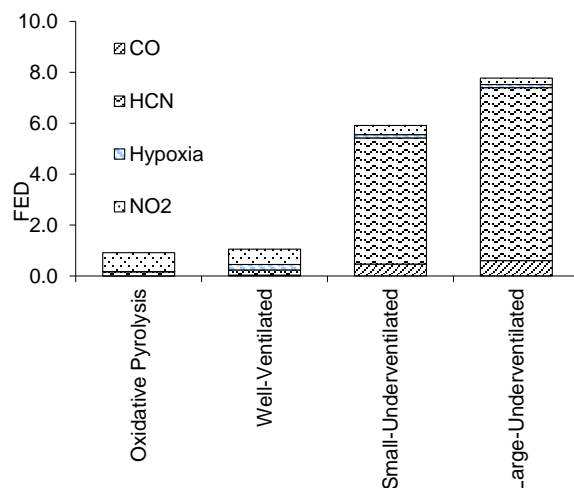


**Figure 2** The contribution to toxicity of individual effluent components from polyamide 6 in different fire conditions

This shows that in well-ventilated conditions, ( $\phi \ll 1.0$ ) the toxicity is low. For under-ventilated conditions ( $\phi > 1.0$ ), the most significant contribution to the toxicity comes from HCN.

## 1.4 Fire Hazards relating to electrical and electronic applications

Glass reinforced polyamides are particularly common in electrical connectors and fuse boxes. The hazards presented by fire in electrical and electronic applications are rather different to those of larger or bulkier items, such as upholstered furniture or flammable insulation materials [15]. In the latter cases, once ignition occurs, fire growth will be rapid until it is controlled by the availability of oxygen, when it will continue to burn with  $\phi > 1$ . In contrast, electrical and electronic components are at a higher risk of ignition due to the heating properties of electric currents, often under forced ventilation, but individual units tend to be smaller and better separated from other sources of fuel. Thus, while the under-ventilated fire is the most likely scenario for fire hazard assessment involving upholstered furniture, for a fuse box, or connector, it is more appropriate to focus on the fire toxicity in well-ventilated conditions.

## 1.5 Flammability and fire toxicity regulation

In Europe, the fire safety requirements for connectors and switches include IEC 60898 for circuit breakers, IEC 60947 for industrial control equipment and IEC 60335 for domestic appliances. The US Underwriters Laboratories (UL) standards have been widely adopted in Europe and Asia, as a material flammability classification test. UL 94 V-0, for example, is probably the most commonly used requirement for reduced flammability across the globe.

The fire toxicity of components is specifically regulated in high risk applications, such as the mass transport industries (rail, air and sea), and in building regulations in China and Japan. In addition, performance based codes, used to produce a more holistic approach to fire safety, require quantification of available safe escape time (ASET) [13], before escaping is impeded by smoke, irritant gases or asphyxiants.

## 1.6 Polyamide materials for electrical and electronic applications

Polyamides are often chosen for electrical connectors and switch housings because of their toughness and rigidity. They are frequently reinforced with glass fibres to enhance their strength and dimensional stability. In connectors, polyamides permit the use of so-called “living hinges”, thin plastics that can be flexed repeatedly without breaking; toughness is particularly important in snap-fits for terminal blocks to allow easy assembly. Polyamides also have good heat-ageing properties, which is important because of the increasing temperatures due to miniaturization of electrical components and devices. However, these excellent mechanical properties are offset by fairly high flammability. Therefore, in many applications, a fire retardant must be added to the polymer.

## 1.7 Fire retardation of polyamides

The physical properties of glass fibre reinforced polyamides make them suitable for electrical devices with applications using high voltages. In polyamides, during burning, the glass fibre acts to stabilise the char [16]. However, regulatory requirements demand low flammability for materials in such applications. Flame retardants added to meet demanding requirements such as the UL-94 V-0 classification must not adversely affect the physical properties, or the durability of electrical components. Glass fibre reinforced polyamide 6 and 6.6 can be effectively flame retarded with

halogenated flame retardants, such as brominated polystyrene, often used in combination with a synergist of antimony oxide, or with salts of organic phosphinic acids. The efficiency of dialkyl phosphinic acids as flame retardants in polyamides has been improved by synergism with melamine polyphosphate (MPP), achieving UL94 V-0 in glass filled polyamides [17]. The combination of diethyl aluminium phosphinate (ALPi) and MPP allows the loading in PA 6.6 to be reduced from 30% (for ALPi alone) to around 15-20%, and still meet regulatory requirements, such as UL94 V-0 at thicknesses as low as 0.8 mm [16]. The mechanism of fire-retardant action of these phosphinic salts is considered in more detail in the discussion.

Halogenated flame retardants have a significant share of the market in reinforced polyamide mouldings, although competition from commercially available mixtures of the aluminium salt of diethyl phosphinate with melamine polyphosphate is growing.

### **1.8 Drivers for the replacement of brominated flame retardants**

The development of halogen-free fire retardant systems has been driven by environmental arguments, which have had surprisingly little airing within the fire retardant polymer community, although we are all busy developing halogen-free fire retardant systems. Several halogenated flame retardants have been shown to be persistent and bioaccumulative, and are now ubiquitous throughout the built and natural environment [18, 19]. A number of detailed studies have demonstrated the toxicity of these releases to humans and animals [20]. In 2010, a group of over 200 concerned scientists signed the San Antonio statement on brominated and chlorinated flame retardants [21] questioning their continued use and requesting urgent remedial action. The flame retardants currently causing concern are small molecules which can easily migrate through the polymer matrix, with consequent release into the environment. The brominated polystyrene used in this study is considered insufficiently mobile for release and transport in the environment. Further, there are now concerns over the fate of the halogen flame retardant synergist, antimony oxide, which has similar toxicity to arsenic oxides, with a threshold limit value of  $0.5 \text{ mg/m}^3$ , in common with most antimony compounds [22]. Currently, (2013) though its high price (around  $\text{€}10 \text{ kg}^{-1}$ ) is also prompting searches for its replacement. Its persistence and toxicity mean that it is also considered a substance of environmental concern.

## **2 Experimental**

### **2.1 Sample preparation**

Six glass-reinforced polyamide materials were investigated, three based on polyamide 6, and the other three on polyamide 6.6. For simplicity, these glass fibre composites will simply be referred to as PA 6 or PA 6.6. Each of these glass fibre composites was flame retarded using standard industry formulations containing either a blend of aluminium phosphinate and melamine polyphosphate (collectively abbreviated to ALPiM) or brominated polystyrene and antimony oxide (abbreviated to BrSb). All the flame retardant samples were formulated to meet UL-94 V-0 at 0.8 mm. In practice, this required a total flame retardant loading was lower for the PA/ALPiM materials than for the PA/BrSb materials. The percentage by weight of each component is shown in Table 2.

Compounds were prepared using a Leistritz ZSE 27 HP 44D twin screw extruder with a screw speed of 200 rpm (20 kg h<sup>-1</sup>). Extruded materials were water cooled and pelletized with a rotary cutter mill. The granulates were dried prior to being tested in the SSTF.

**Table 2 Sample composition and abbreviated descriptor**

Descriptor						
Component	PA6	PA6/AlPiM	PA6/BrSb	PA6.6	PA6.6/AlPiM	PA6.6/BrSb
PA 6	69.7	49.7	43.7			
PA 6.6				69.7	49.7	43.7
Glass fibre	30	30	30	30	30	30
Processing aid	0.3	0.3	0.3	0.3	0.3	0.3
Aluminium phosphinate/ Melamine polyphosphate		20			20	
Brominated polystyrene			20			20
Antimony trioxide			6			6

The product names (manufacturer) of the individual components are: PA 6, Durethan B29 (Lanxess); PA 6.6, Ultramid A27 (BASF); glass fibre, ESC-301CL (length 4.5 mm, diameter 10 µm) (CIPC); aluminium phosphinate, Exolit OP 1230 (Clariant); melamine phosphate, Melapur 200/70 (BASF); brominated polystyrene, Saytex HP 3010G (Albemarle); Antimony Trioxide (as masterbatch in PA 6) 2617 (Campine); processing aid, Licowax E (Clariant).

## 2.2 Steady state tube furnace apparatus (ISO/DIS 19700)

The steady state tube furnace apparatus has been described elsewhere [11, 23], and is shown in Figure 3.

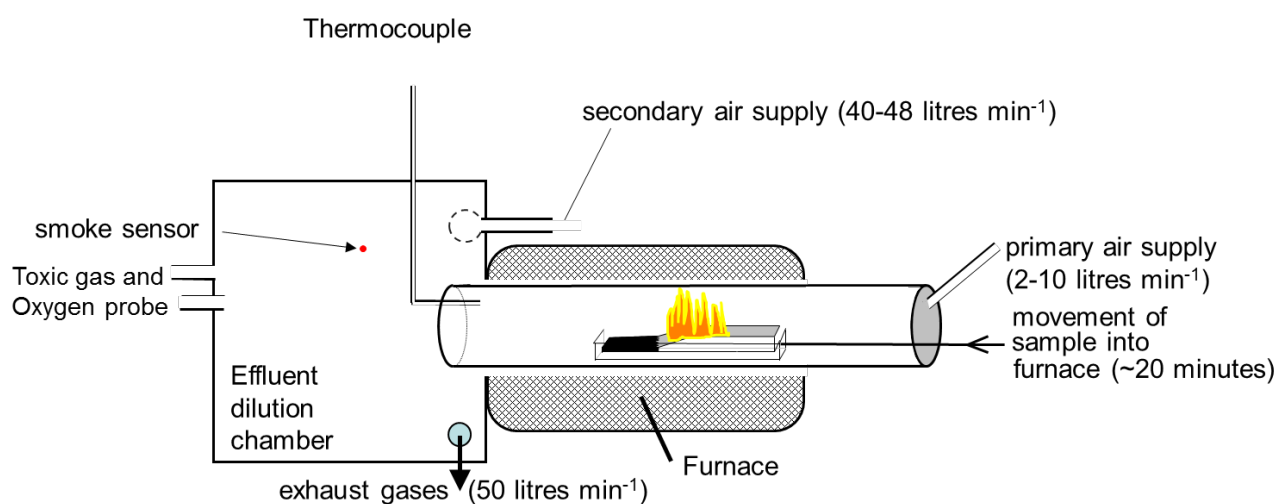


**Figure 3 Diagram of the steady state tube furnace (ISO TS 19700)**

The apparatus consists of a stationary tube furnace in which a quartz tube is fixed. Granules of the test specimen were placed in an 800 mm silica boat. During each experiment, the boat is driven into

the furnace at a constant and controlled flow rate around  $1 \text{ g min}^{-1}$ , typically over a period of about 20 minutes. A fixed flow of primary air passes through the tube furnace where it can react with the pyrolysing polymer, ignite and the gas phase fuel mix with all the available oxygen in the tube, and the resulting fumes pass into the effluent dilution chamber where it is mixed with a fixed and controlled secondary air supply. The secondary air increases the volume of analyte, and tends to keep the effluents from different ventilation conditions within the same analytical range. The requirement in each test run is to obtain a steady state of at least 5 minutes during which the concentrations of effluent gases and particulates can be measured, and flaming (or non-flaming) can be observed. For materials which do not burn completely, such as those containing non-combustible fillers, forming a char or leaving a residue, and those of unknown composition, the equivalence ratio can only be determined by calculating the oxygen depletion after the experiment. In this work, the primary air flow was varied with a fixed fuel feed rate in order to vary the equivalence ratio.

### 3 Results

The experiments were performed on granulated materials for a well-ventilated fire scenario at furnace temperatures of 650 and 850 °C. The actual equivalence ratio was obtained after subtraction of the mass of residue at the end of the experiment. This introduced a relatively small perturbation in the test conditions, which was not apparent until the end of the test (section 2.2). Carbon monoxide and carbon dioxide yields were measured together with hydrogen cyanide, nitrogen dioxide and hydrogen bromide. The yields are all expressed on a mass-charge basis, and yields and measured equivalence ratios from comparable runs are presented individually, showing the actual values of the equivalence ratio.

#### 3.1 Polyamide 6

The yields of carbon dioxide, carbon monoxide, hydrogen cyanide and nitrogen dioxide are presented for each polyamide as representative of the toxicants present. For the two materials containing bromine (PA 6/BrSb and PA 6.6/BrSb), data on HBr yields is presented at the end of the section on Polyamide 6.6. Only one result was obtained for well-ventilated conditions for PA 6/BrSb at 650 °C, but results are also shown for  $\phi$  values around 1, which suggest similar trends with the single exception of the HCN yield for PA 6/BrSb at 650 °C



### 3.1.1 Carbon dioxide yields

Figure 4 shows the variation in carbon dioxide yields for the three polyamide 6/glass fibre based materials. This can be related to the combustion efficiency. The theoretical maximum CO<sub>2</sub> yield from complete combustion of PA 6 containing 30% glass fibres is 1.64 g CO<sub>2</sub> per g of material. Thus the PA 6 is burning with around 85 % combustion efficiency at 650 °C and, surprisingly, around 80 % at 825 °C. The PA 6 sample flame retarded with aluminium phosphinate and melamine polyphosphate (PA 6/AlPiM) has a theoretical yield of 1.4 g CO<sub>2</sub> per g of material, showing a disproportionately lower CO<sub>2</sub> yield than PA 6, indicating both the lower carbon content, and a reduced combustion efficiency, indicative of gas phase inhibition. There is little difference between the yields at 650 °C and 825 °C. The PA 6 sample flame retarded with brominated polystyrene and antimony trioxide (PA 6/BrSb) with a theoretical yield of 1.3 g CO<sub>2</sub> per g of material, shows lower combustion efficiency and hence considerable gas phase inhibition at 650 °C, though the combustion efficiency increases noticeably at 825 °C.

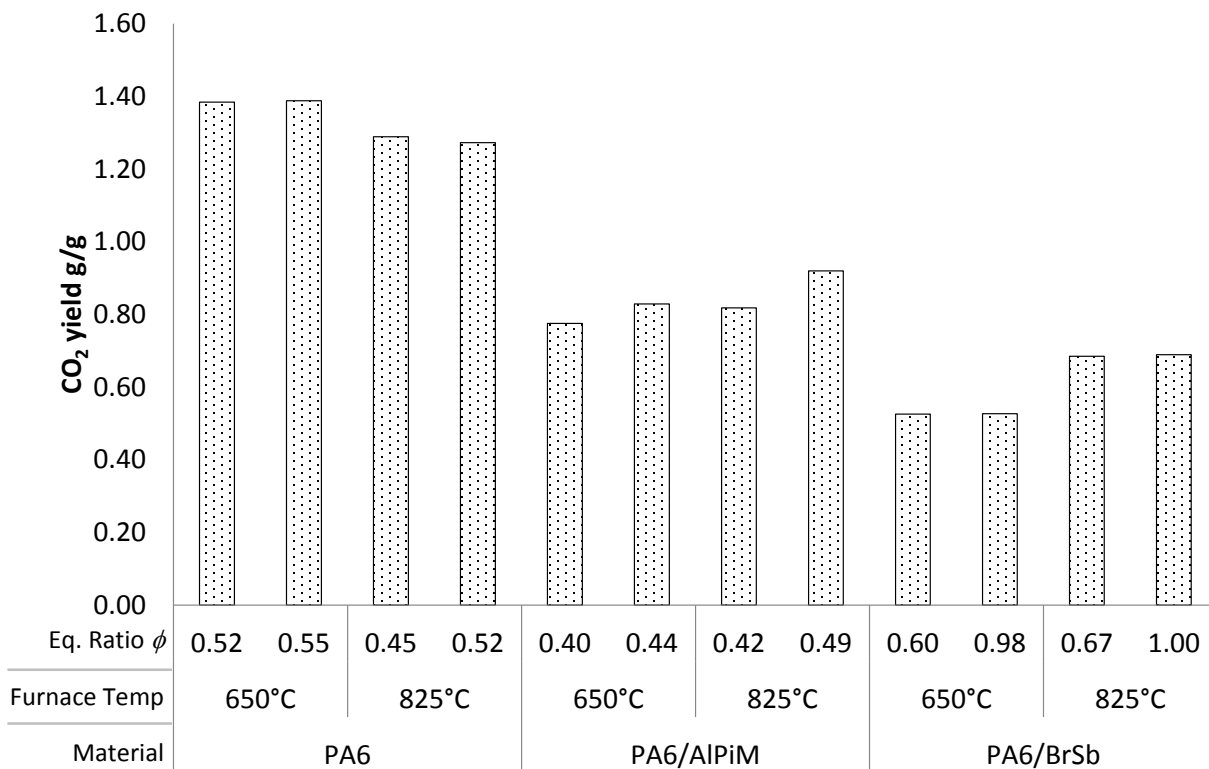


**Figure 4 Carbon dioxide yields from PA 6 based materials**

### 3.1.2 Carbon monoxide yields

As well as being a toxicant in its own right, carbon monoxide is generally considered a good indicator of incomplete combustion. Thus if the CO yield is high, it is likely that the yields of the other toxic products will also be higher. Figure 5 shows the CO yields from PA 6 materials. PA 6 shows low CO yields at both 650 and 825 °C. In contrast, PA 6/AIPiM shows elevated CO yields at 650 °C, which are not observed for the same material burnt at 825 °C, suggesting gas phase inhibition occurs at 650 °C, but is “switched off” at 825 °C. The slight increase in CO<sub>2</sub> yields at 825 °C is more than sufficient to account for this change. For the PA 6/BrSb material, the CO yield is very high, particularly at 650 °C, though in both cases only showing a small increase with increase in  $\phi$ . Given the lower fuel content of PA 6/BrSb (containing both GF, brominated polystyrene and antimony oxide) this yield, per g of PA 6, is higher than that for pure polyamide 6 (Figure 1) under the most toxic, underventilated conditions. This shows gas phase inhibition of the conversion of CO to CO<sub>2</sub>, which is not sensitive to temperature over the range considered.

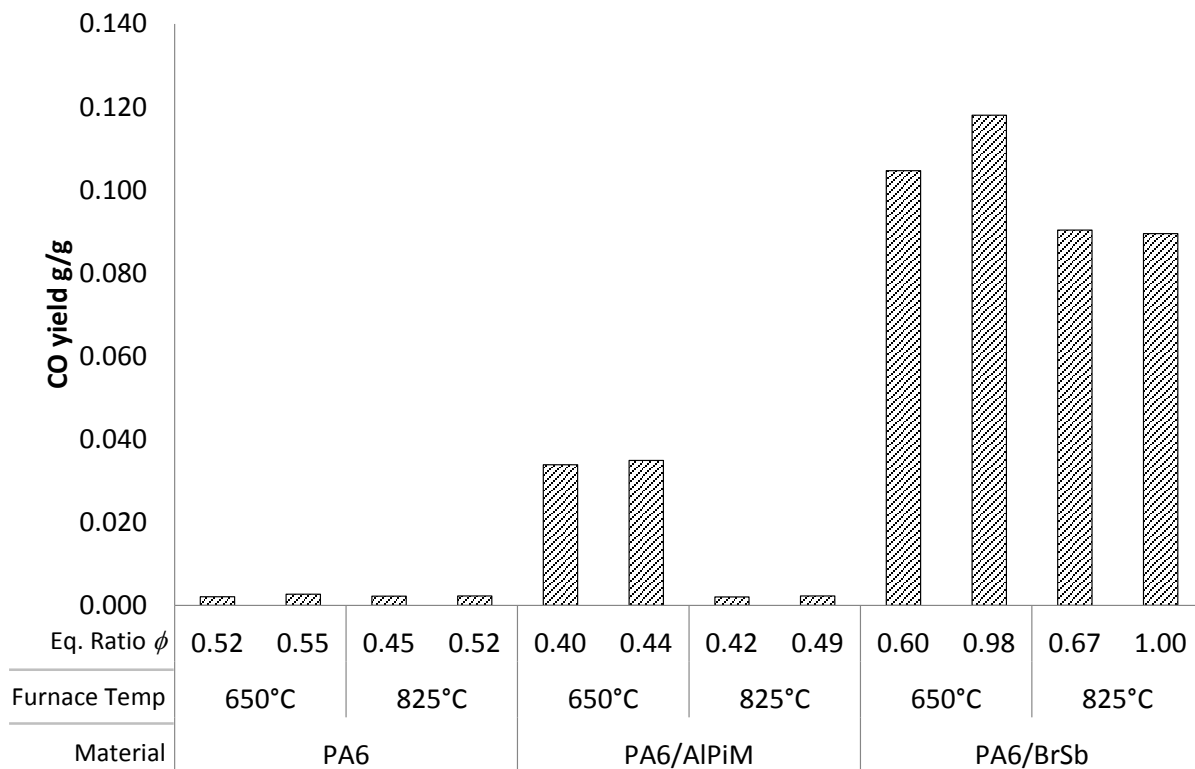


**Figure 5 Carbon monoxide yields from PA 6 based materials**

### 3.1.3 Hydrogen cyanide yields

The hydrogen cyanide yields for a related polymer, polyamide 6.6 are described in the introduction, and only show significant yields in under-ventilated conditions. Figure 6 shows the HCN yields for the three PA 6 materials. It can be seen that very low, but measurable yields of HCN are observed for PA 6 with glass fibre. As the furnace temperature increases from 650 to 825 °C, there is a noticeable decrease in the HCN yield, showing more complete oxidation. A higher HCN yield is observed for the PA 6/AlPiM material, indicative of gas phase inhibition, which switches off at 825 °C, when the HCN yield falls by over 50 %. In contrast, the HCN yield from the PA 6/BrSb material is around a factor of 20 greater than that for PA 6, and around a factor of 5 greater than that from PA 6/AlPiM. In addition, at the lower furnace temperature, the HCN yield is more strongly dependent on equivalence ratio, whereas at the higher temperature, it is almost independent of equivalence ratio. Most notably, in well-ventilated conditions, when little HCN is produced by non-flame retardant polyamides, the material containing BrSb shows the highest CO and HCN yields of any of those tested.

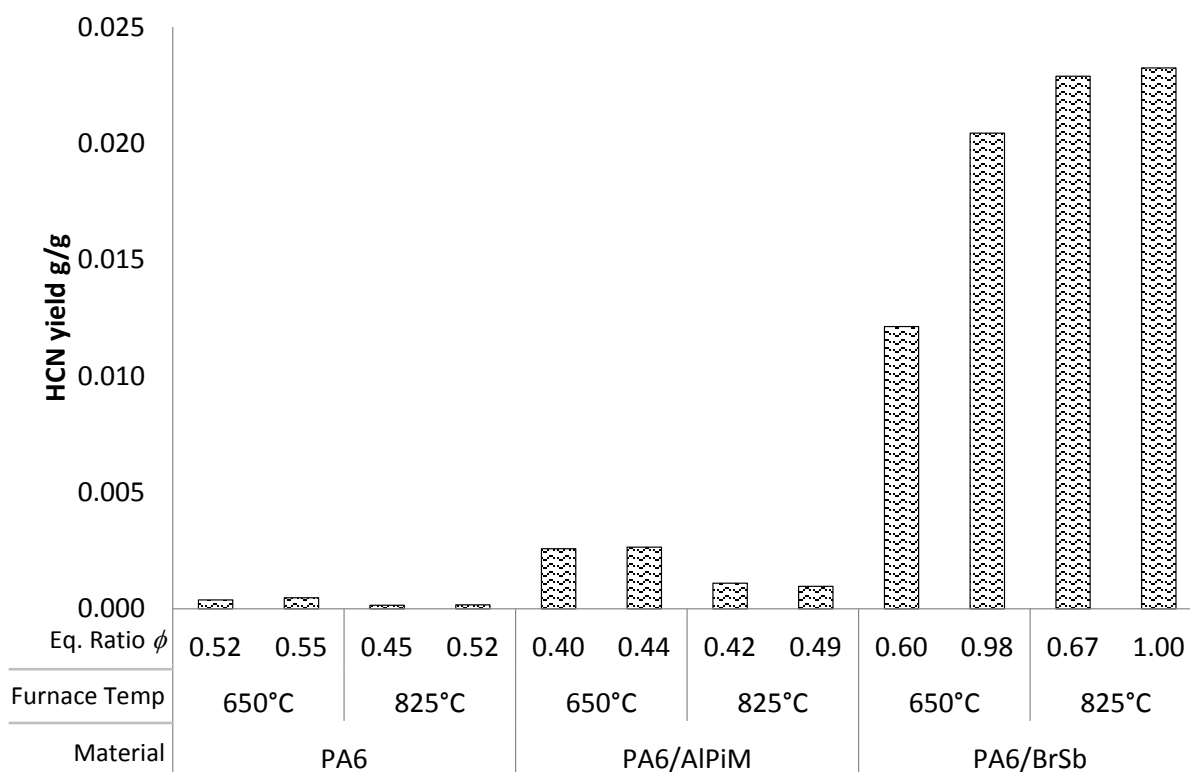


**Figure 6 Hydrogen cyanide yields from PA 6 based materials**

### 3.1.4 Nitrogen dioxide yields

Very low yields of nitrogen dioxide were found during combustion of the PA 6 based materials. The  $\text{NO}_2$  detected is close to the limits of detection and quantification. Figure 7 shows the variation of  $\text{NO}_2$  yields for the three PA 6 materials. There seems to be a progressive increase in  $\text{NO}_2$  yields with gas phase inhibition, surprisingly showing a similar trend to the CO and HCN yields.

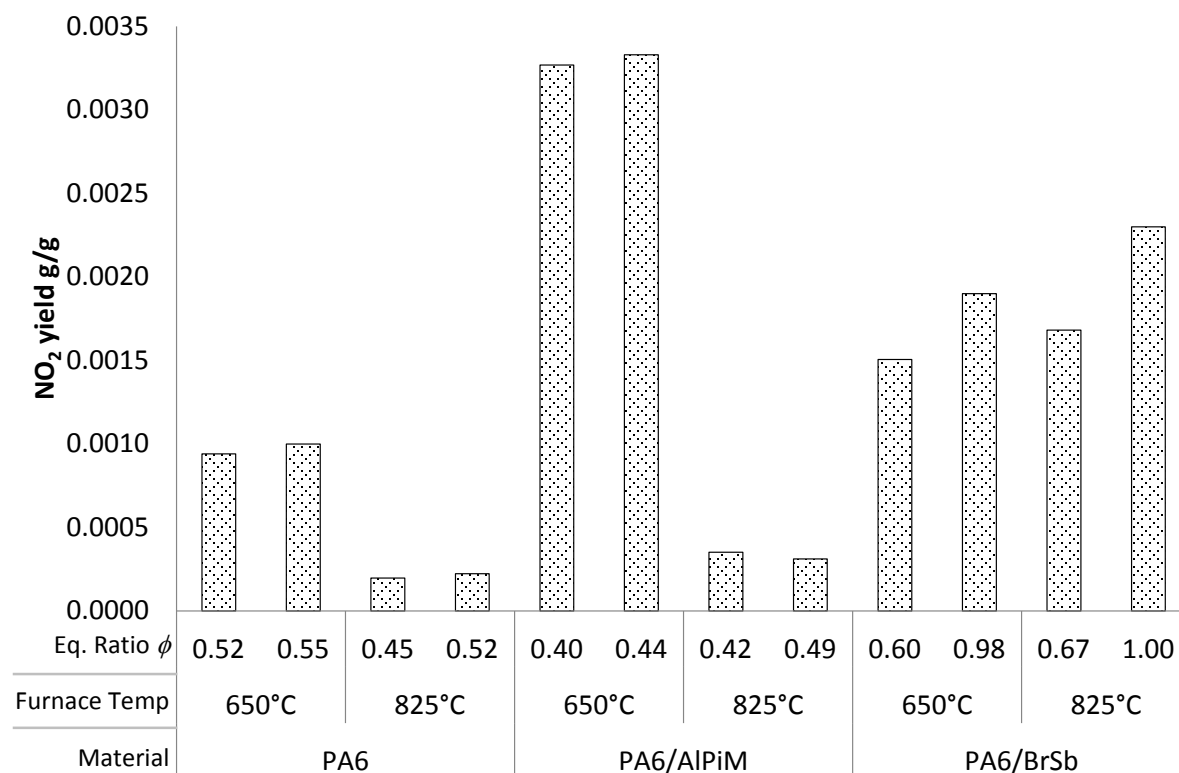


Figure 7  $\text{NO}_2$  yields from PA 6 based materials

## 3.2 Polyamide 6.6

The results for glass-reinforced polyamide 6.6 based materials show similar trends to those observed for PA 6.

### 3.2.1 Carbon dioxide yields

The theoretical yield of CO<sub>2</sub> for complete combustion of PA 6.6 containing 30% glass fibre is 1.57 g/g. The measured yields, shown in Figure 8, are similar to those for PA 6, showing high combustion efficiency. For PA 6.6/AlPiM, with a theoretical yield of 1.33 g CO<sub>2</sub> per g of material burnt, the lower combustion efficiency observed at 650 °C is less evident at 825 °C. For PA 6.6/BrSb, with a theoretical yield of 1.26 g CO<sub>2</sub>, a very low combustion efficiency is observed at 650 °C, which shows only a small increase at 825 °C, suggesting the antimony-bromine combination is a more efficient gas phase inhibitor for PA 6.6 than for PA 6.

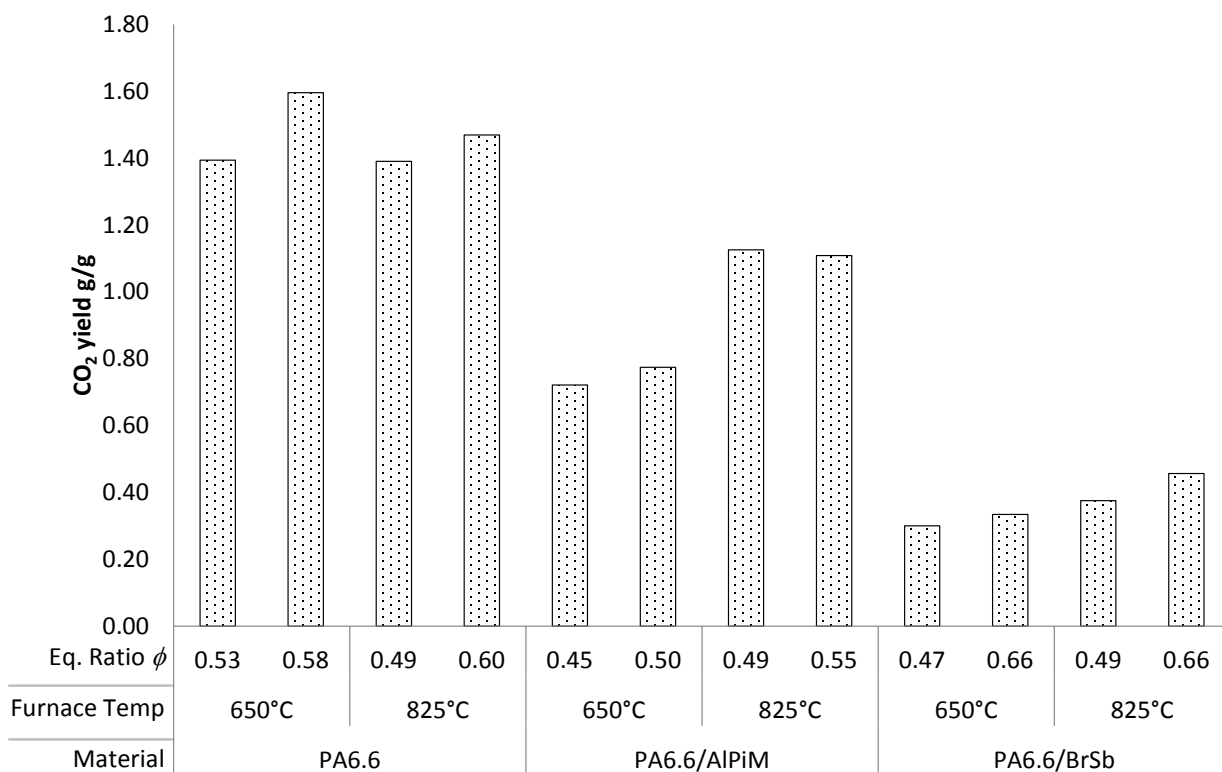
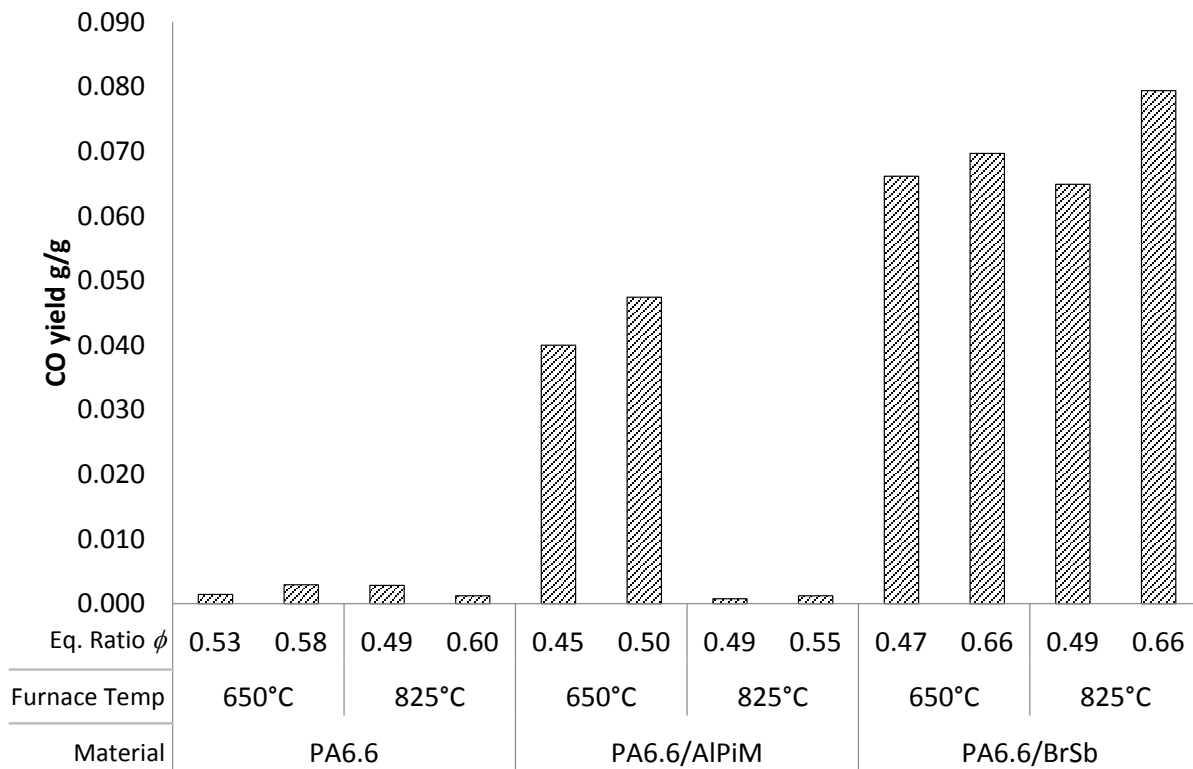


Figure 8 Carbon dioxide yields from PA 6.6 based materials

### 3.2.2 Carbon monoxide yields

The CO yields for PA 6.6 based materials are shown in Figure 9. PA 6.6 alone shows low CO yields, confirming the high combustion efficiency at both 650 and 825 °C observed for the CO<sub>2</sub> yields. For PA 6.6/AlPiM, similar behaviour is observed to the PA 6/AlPiM material, except that the difference between the two furnace temperature settings appears to be even greater. At 650 °C, the CO yield is higher for PA 6.6 than for PA 6, while at 825 °C, it is lower. More noticeable is the dramatic increase in CO yield at both 650 and 825 °C for the PA 6/BrSb material.



**Figure 9 Carbon monoxide yields from PA 6.6 based materials**

### 3.2.3 Hydrogen cyanide yields

The HCN yields for PA 6.6 based materials are shown in Figure 10. For PA 6.6 and PA 6.6/AlPiM, these show a similar trend to those for CO, in that the PA 6.6 yields are very low, and the PA 6.6/AlPiM yields decrease from 650 to 825 °C. The HCN yields from the PA 6.6/BrSb material are very high yield for burning in well-ventilated conditions. Moreover, as observed for the CO yield for the PA 6.6/BrSb, there appears to be a slight increase in the HCN yield (and hence the inhibitory effects of brominated polystyrene and antimony oxide) at 825 °C.

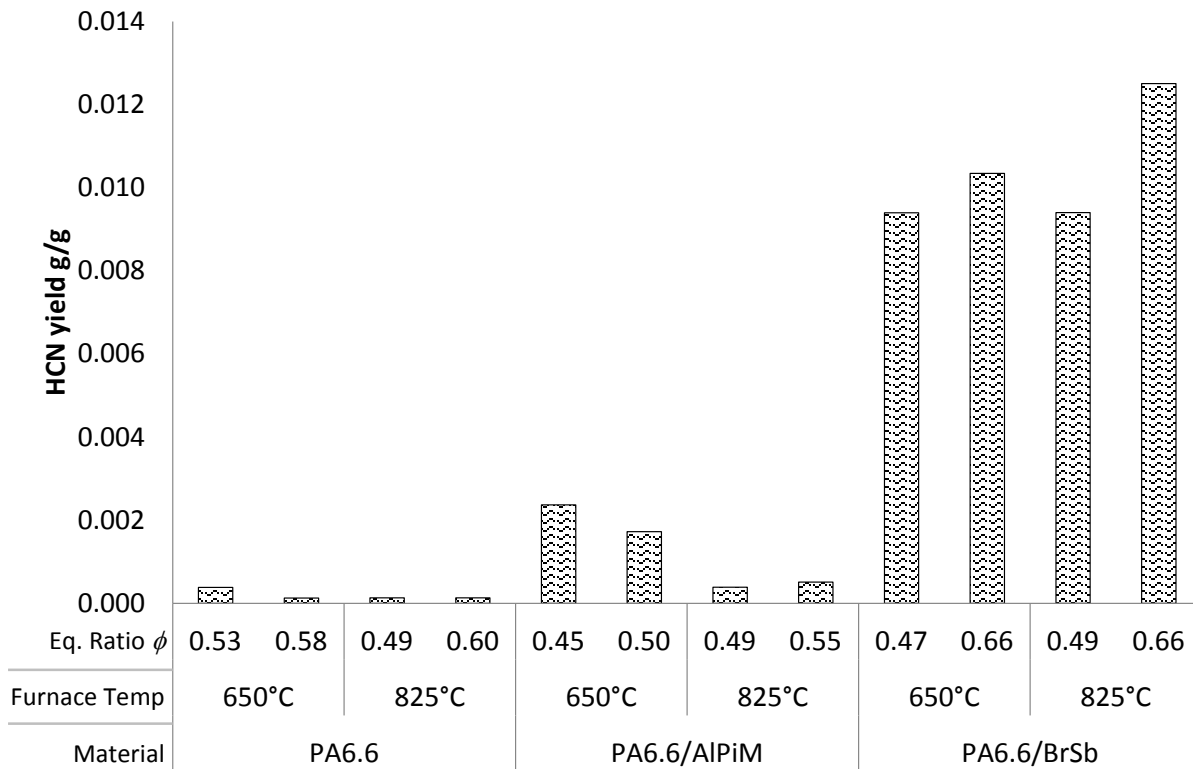


**Figure 10 Hydrogen cyanide yields from PA 6.6 based materials**

### 3.2.4 Nitrogen dioxide yields

Figure 11 shows the NO<sub>2</sub> yields for PA 6.6 based materials. Again all the yields are close to the limits of detection and quantification, though higher than those for PA 6. Similar to PA 6 materials, the highest NO<sub>2</sub> yields are found for PA 6.6/AlPiM materials burnt in the furnace at 650 °C. A similar, but smaller trend of NO<sub>2</sub> formation being favoured at lower furnace temperatures appears to be evident from the PA 6.6/BrSb materials burnt at the lower temperature in the more well-ventilated condition of  $\phi = 0.47$ .

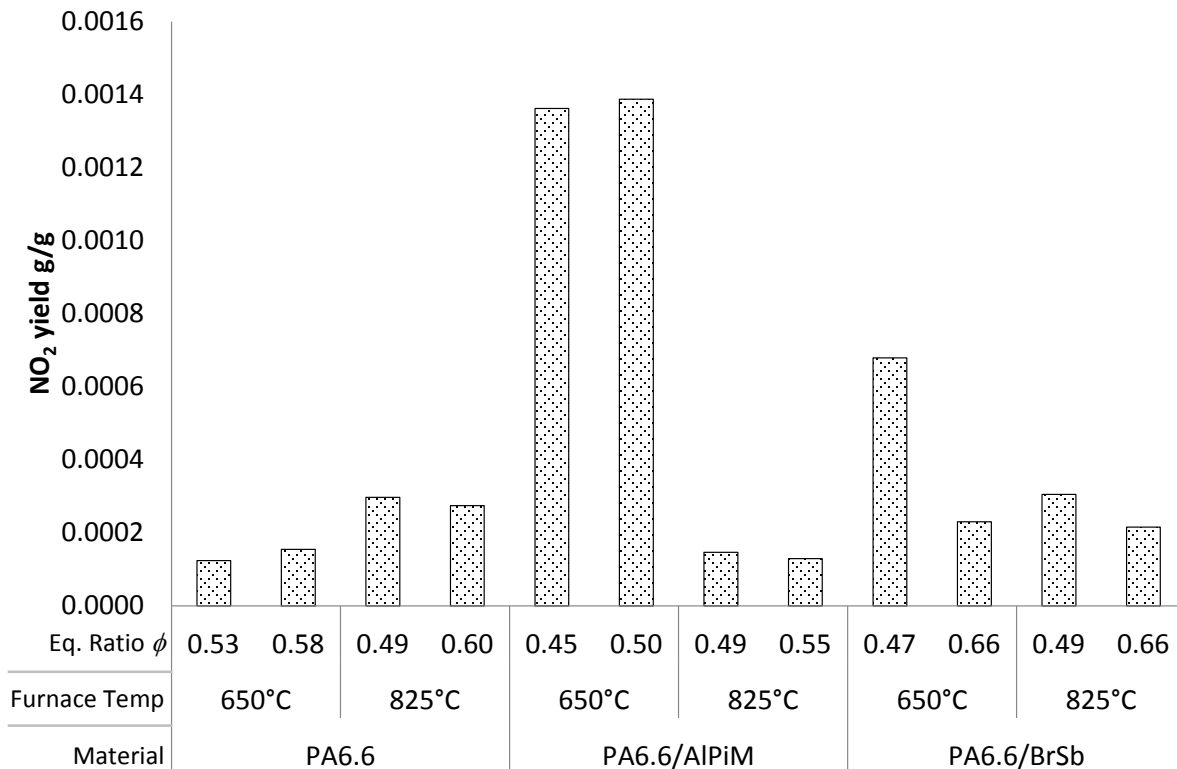


Figure 11 NO<sub>2</sub> yields from PA 6.6 based materials



### 3.2.5 Hydrogen bromide yields from PA 6/BrSb and PA 6.6/BrSb

Figure 12 shows the measured yield of hydrogen bromide (HBr) from the materials containing the brominated polystyrene flame retardant. The theoretical yield of HBr is around 0.14 g/g. The maximum recovery of bromine as HBr is thus only around 25% this. This probably arises from the readiness of acid gases to attach themselves to exposed metal surfaces, water droplets and soot particles, and may represent an underestimate of the quantities of HBr that may be encountered in the effluent from a real fire. Alternatively, more bromine may be present in organic form, rather than as HBr, although the high yields of CO, in particular, also suggest a higher concentration of HBr than those detected, since HBr inhibits the conversion of CO to CO<sub>2</sub>, by reducing the ·OH concentration.

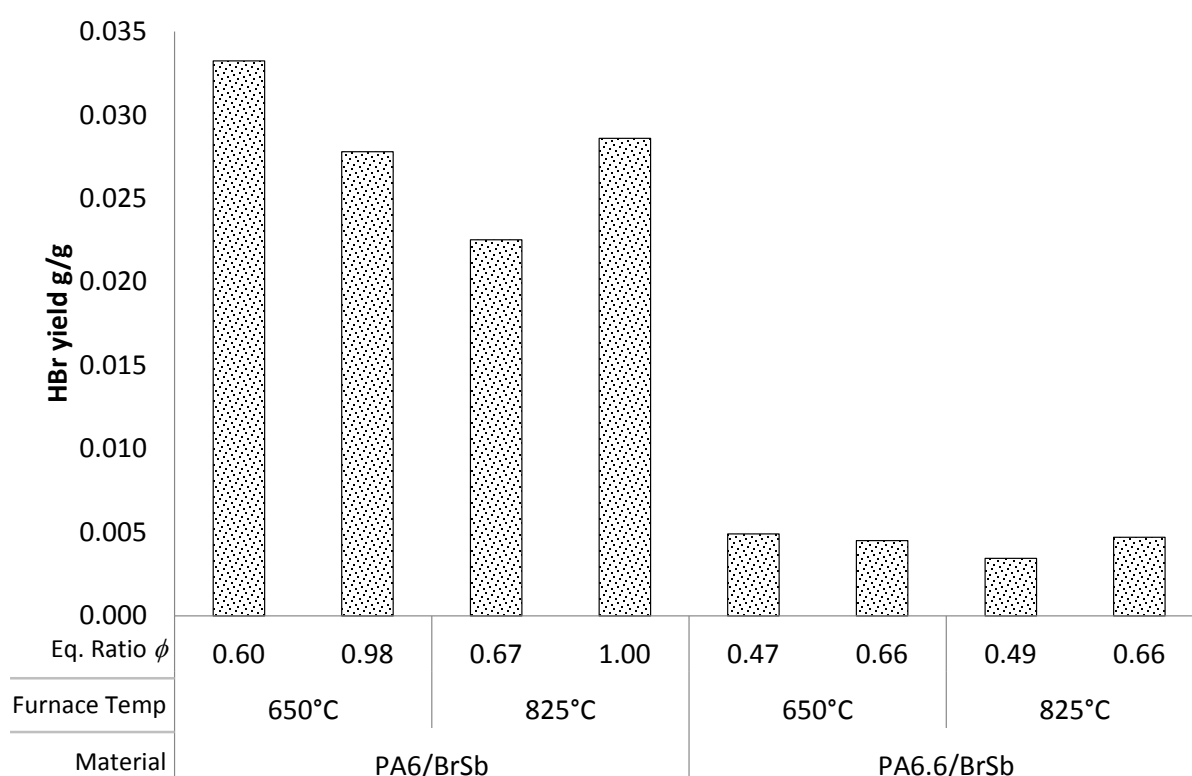


Figure 12 HBr yields from materials containing bromine

## 4 Discussion

This work has shown that in aliphatic polyamides, brominated *flame* retardants with an antimony oxide synergist, which interfere with gas-phase free radical reactions, produce high yields of both carbon monoxide and hydrogen cyanide. In contrast, the aluminium phosphinate/melamine polyphosphate combination, which is believed to act in both gas and condensed phases, causes a significantly smaller increase in the yields of these two main asphyxiants. These yields may be expressed in terms of estimates of effluent toxicity.

### 4.1 Estimation of contribution to toxicity of individual components in the fire effluent

Figure 13 shows how the individual yields may be translated into estimates of toxicity expressed as fractional effective dose (FED), (at an arbitrary loading of 1 kg of material in 50 m<sup>3</sup>). Even at this high loading, many of the material/conditions show FEDs well below the critical value of 1 (representing lethality to 50 % of the population during a 30 minute exposure). The two exceptions are the materials containing AlPiM, when burning at the lower furnace temperature of 650° C, and the materials containing BrSb at both furnace temperatures. In each case, where the FEDs exceed one, the major contribution to the toxicity comes from hydrogen cyanide, with smaller contribution from carbon monoxide at about 1/5<sup>th</sup> of the HCN level. There is also a minor contribution from NO<sub>2</sub> from all materials, in all fire conditions. It is notable that the fire toxicity of the PA 6/BrSb materials is a factor of 10 larger than that of PA 6 and a factor of 5 larger than the AlPiM material at 650° C; at 825° C it is a factor of 30 larger than the PA 6, and 17 larger than the AlPiM material. The BrSb materials all show high fire toxicity under the normally least toxic, well-ventilated fire conditions. The lower fire toxicity of the AlPiM materials at higher temperatures suggest a reduction in fire hazard. It is well known that under more severe conditions than a small flame ignition test, flame retarded materials will burn, and frequently produce more toxic effluents as a result of quenching of the gas phase flame reactions. It appears that the AlPiM system switches off this flame quenching process as the fire becomes more severe, reducing the toxicity of the effluent. These surprising findings led to the detailed investigation of the chemistry of the processes, which are discussed in more detail in 4.2.

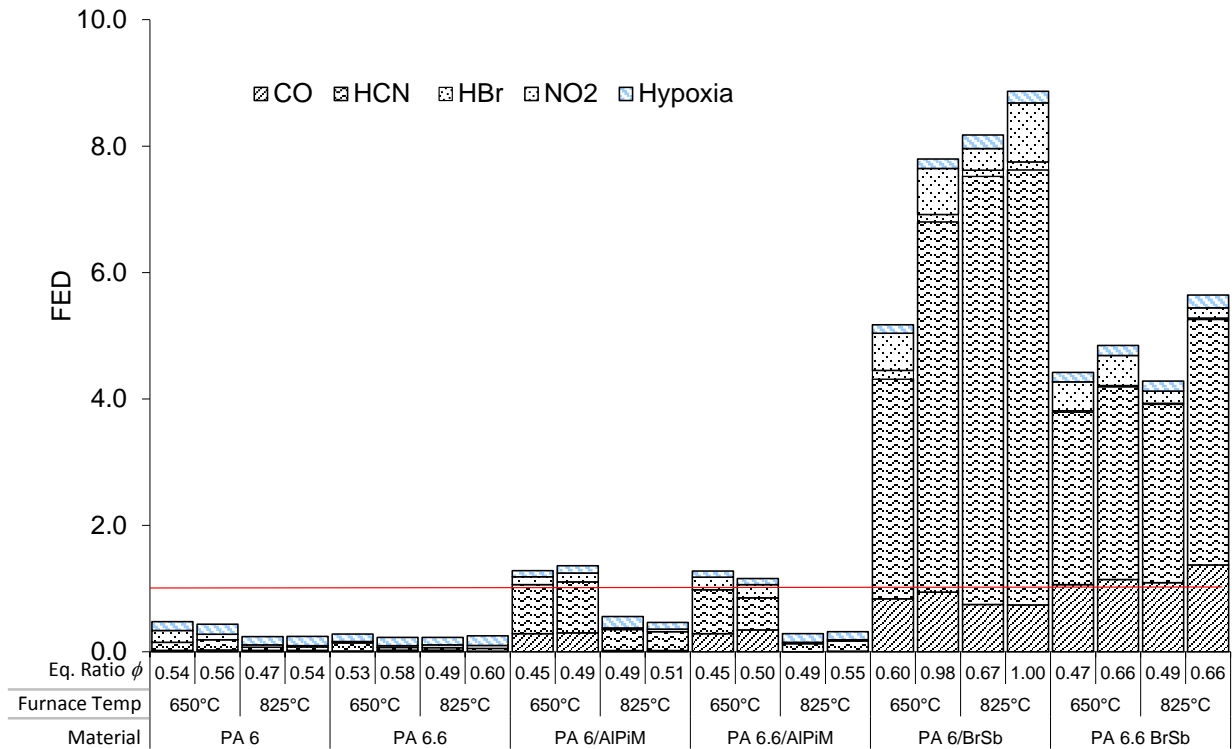


**Figure 13 Contributions to effluent toxicity from PA 6 and PA 6.6 based materials**

These estimates of toxicity can be expressed in terms of fire safe limits on combustible loadings in enclosures. The  $LC_{50}$  concept may also be applied to materials burning under specified conditions. In this case, the  $LC_{50}$  is related to the FED by Equation 3 [12].

$$LC_{50} = \frac{m}{V \times FED}$$

**Equation 3**

Thus for the base polymers with glass fibre reinforcement, and for the four comparably flame retarded samples, an  $LC_{50}$  may be calculated (

Table 3).

**Table 3  $LC_{50}$  for each material and furnace temperature (the mass required to generate a lethal effluent in grams per cubic metre)**

Sample	Furnace Temperature /°C	
	650	825
PA 6	44	83
PA 6/AlPiM	15	40
PA 6/BrSb	3.3	2.4
PA 6.6	80	84
PA 6.6/AlPiM	16	66

PA 6.6/BrSb	4.3	4.1
-------------	-----	-----

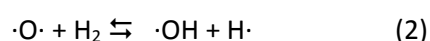
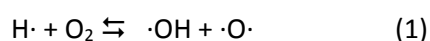
The LC<sub>50</sub> is inversely proportional to the toxicity (higher values indicate lower toxicity). If the mass of material equal to the LC<sub>50</sub> is burnt in well-ventilated conditions, this would be fatal to 50% of the occupying population. Therefore, if a 1 kg fuse box made of glass reinforced polyamide 6, flame retarded to UL94 V-0 with brominated polystyrene and antimony oxide, was to burn completely in conditions corresponding to a small, well-ventilated fire (650° C) it would generate a volume of lethal effluent of 300 m<sup>3</sup> (for 30 min exposure), whereas if it were flame retarded with ALPiM it would only generate a volume of lethal effluent of 67 m<sup>3</sup> under the same conditions. Fire safety engineers would generally apply a safety margin, for example that the FED could not exceed 0.3, to ensure that the fire effluent would not be lethal to the occupying population.

## 4.2 Gas phase flame retardant mechanisms

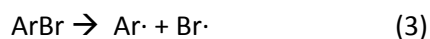
Both carbon monoxide and hydrogen cyanide are formed in the flames of burning polyamides (and other polymers containing C and N). The effects of brominated and phosphinate flame retardants on these processes are considered, in order to explain why the ALPiM flame retardant had a lesser effect on the yields of CO and HCN, and their sensitivity to furnace temperature.

## 4.3 Flame retardant mechanism of antimony-bromine systems

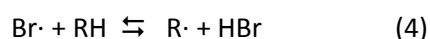
Flaming combustion involves a complex set of reactions between a very small number of highly reactive free radicals. For ignition to occur, the number of radicals must exceed a small, but critical concentration. In reactions 1 and 2, each “·” represents an unpaired electron; overall, the reaction of a single H· radical with molecular oxygen results in the formation of three radicals. This is the “chain-branching” step fundamental to all flaming reactions.



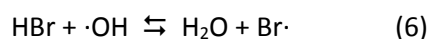
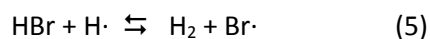
Once sufficient radicals have been formed, their concentration needs to be maintained for flaming combustion to continue. In the gas phase, brominated flame retardants act by releasing hydrogen bromide (HBr) during thermal decomposition, which interferes with the flame processes. During polymer decomposition, the flame retardant (such as brominated polystyrene) breaks down.



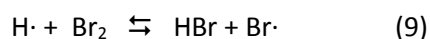
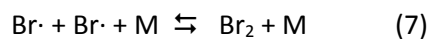
The bromine radical abstracts H· from a fuel molecule to form HBr:



which in turn interferes with the radical chain mechanism:



Thus the high-energy OH· and H· radicals formed by chain branching are removed by the HBr. The removal of H· is key to elimination of the main chain branching steps (1 and 2) (when 1 radical becomes 3 radicals), preventing the formation of 2 ·OH radicals. Collision with a third body, M, results in termination processes, and crucially, recycling of HBr.



Thus HBr is a catalyst for the recombination of H· atoms (5).

The removal of OH·, by replacement with the less reactive Br·, blocks the main heat release step of hydrocarbon combustion, the conversion of CO to CO<sub>2</sub> (10) [24].



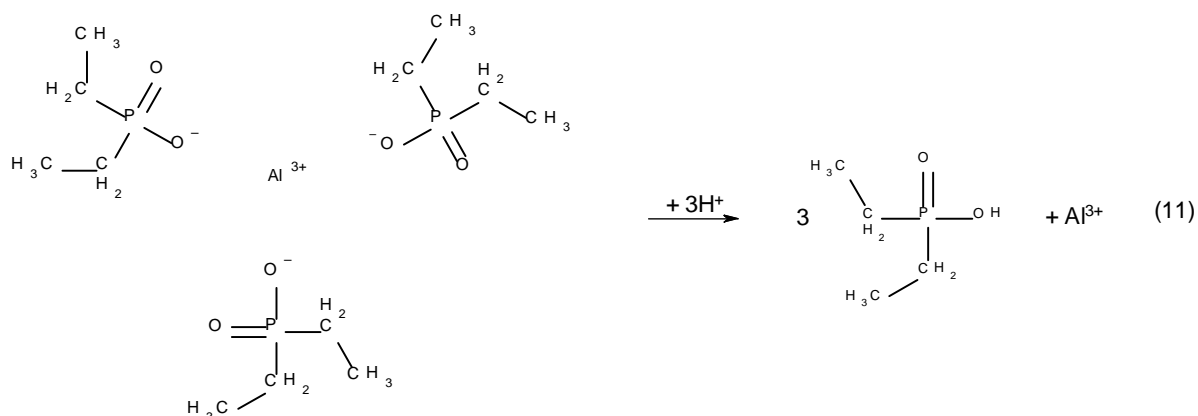
Thus, loss of H· and OH· will increase the yield of carbon monoxide and other products of incomplete combustion. The H· and ·OH radicals are also essential for many other flame reactions.

Kinetic reaction schemes predict that HBr must be recycled around 7 times in order to account for the observed flame inhibition [25]. Thus the hydrogen halide is regenerated by further reaction with another fuel hydrocarbon (4).

In the presence of antimony oxide (Sb<sub>2</sub>O<sub>3</sub>), the efficiency of halogenated flame retardants is significantly improved, although antimony has no flame retardant effect on its own. SbBr<sub>3</sub> is believed to form via the intermediate SbOBr. Sb<sub>2</sub>O<sub>3</sub> and HBr first yield SbOBr, which gives off SbBr<sub>3</sub> over a relatively wide temperature range. The individual endothermic stages ensure that the system is cooled. SbBr<sub>3</sub>, as the actual flame retardant, acts as a radical interceptor like HCl or HBr. It is thought that the trivalent antimony halide facilitates the formation of halogen radicals, and is more effective than HBr [26] at catalysing the recombination of hydrogen.

#### 4.4 Flame retardant mechanism of alkyl phosphinate/melamine polyphosphate systems

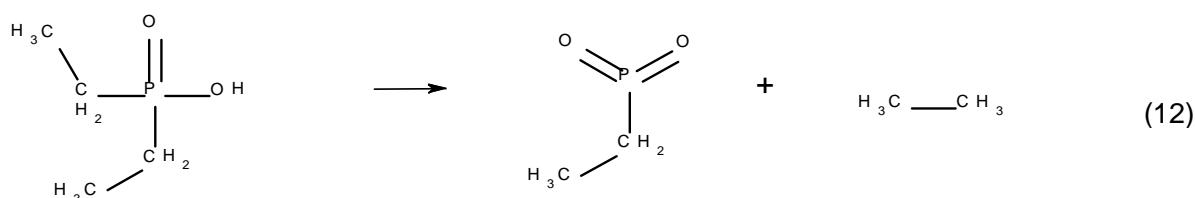
PA 6.6, flame retarded with AlPi decomposes, releasing diethyl phosphinic acid (11); at lower heat fluxes in the cone calorimeter AlPi decomposes in the vapour phase, at higher heat fluxes, diethylphosphinic acid is released from the condensed phase [16].



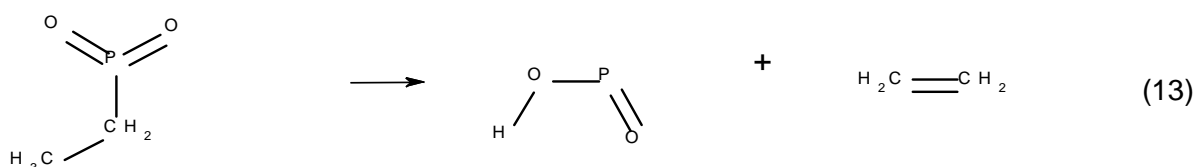
Using similar loadings to the materials in the current study (30% glass fibre but only 18% total fire retardant loading), resulted in residues of 6-8% in addition to glass fibre, when AlPi, MPP or a mixture were present [16]. Moreover, they confirmed the release of diethylphosphinic acid by thermogravimetric analysis, coupled to Fourier transform infrared (TGA-FTIR) ( $3650\text{ cm}^{-1}$  (PO—H),  $1275\text{ cm}^{-1}$  (P=O),  $1243\text{ cm}^{-1}$  (P—C), and  $850\text{ cm}^{-1}$  (P—O)) for both PA 6.6/AlPi and PA 6.6/AlPiM materials. In addition, aluminium phosphates were identified in the residue, and it was assumed that melamine phosphinate may also be present in the vapour [16]. However, a more recent study using TGA FTIR of PA 6 with AlPiM found no evidence for phosphates in the vapour phase under thermo-oxidative conditions [27]. In addition, further details were reported of the contribution made by phosphates to increase the char yield. The increased residue yields incorporating aluminium phosphate [16] and the chemical composition of the residue [27] points to a condensed phase mechanism, whereas the release of diethyl phosphinic acid is strongly suggestive of a gas phase mechanism.

AlPi was shown to reduce the heat release rate of PA 6.6 by inhibition of flaming combustion, while increasing the CO production rate. This gas phase inhibition effect was also evident, but less distinct, for PA 6.6/AlPiM. Thus, both condensed and gas phase mechanisms have been demonstrated.

A related and well-studied gas phase flame retardant, dimethylmethylphosphonate (DMMP) has been reported to decompose via  $\text{CH}_3\text{PO}_2$ . This species was proposed, as a key intermediate in the combustion reactions of DMMP, based on a mass spectrometric investigation ( $\text{CH}_3\text{P}(=\text{O})_2$   $m/z$  78) [28]. This hypothetical structure has been supported by a detailed theoretical investigation using molecular orbital calculations [29]. We propose that AlPi may follow the same pathway, releasing ethane (12).

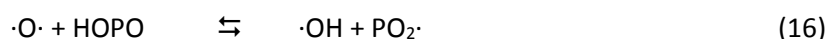
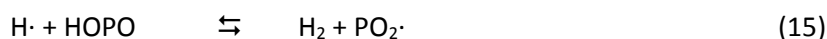
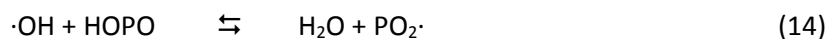


This intermediate decomposes further to generate HOPO and ethane (13).



Ethane and ethene have both been reported in the decomposition of PA 6.6/AlPiM [16]. The *cis*-structure of the HOPO intermediate (13) has been predicted to be the lowest energy isomer, based on molecular orbital calculations [30].

HOPO, HOPO<sub>2</sub>, and the PO<sub>2</sub><sup>·</sup> radical are all known to be very effective free radical trapping agents [31]. Their inhibition of flames has been investigated and modelled by Babushok et al [31]. He has shown that phosphorus containing species such as HPO, PO<sup>·</sup>, PO<sub>2</sub><sup>·</sup>, HOPO and HOPO<sub>2</sub> catalytically recombine H<sup>·</sup> and <sup>·</sup>OH. Since the simple phosphorus-containing species participate in the main inhibition reactions, the form of the parent compound is probably unimportant.



This cycle shows that while H<sup>·</sup> and <sup>·</sup>O<sup>·</sup> are consumed, <sup>·</sup>OH is both consumed and regenerated. Numerical calculations and sensitivity analysis show that the burning velocity is most sensitive to the rate constants of the two recombination reactions of the PO<sub>2</sub><sup>·</sup> radical (reactions 17 and 18).

#### 4.5 Temperature dependence of gas-phase inhibition

Inhibition of flaming combustion by scavenging H<sup>·</sup>, <sup>·</sup>OH and <sup>·</sup>O<sup>·</sup> radicals is temperature dependent. Higher temperatures will generally lead to an increase in all free radical concentrations, from entropy considerations.

A preliminary study [32] in the SSTF using the same PA 6/BrSb formulation reported here showed a modest reduction of CO yield at a furnace temperature of 825 °C, and a large reduction at 950 °C, in well-ventilated conditions. A related SSTF study on the CO yield from PVC (where CO formation is believed to be inhibited by Cl<sup>·</sup> radicals) also showed a significant reduction in CO yield at 950 °C, again, under well-ventilated conditions [33].

The current work in the steady state tube furnace showed a reduction in gas phase inhibition by phosphorus at higher furnace temperatures. Gas phase inhibition was also reduced at higher applied heat fluxes in the cone calorimeter [16]. Assuming that the higher heat fluxes give rise to higher temperatures in the gas phase, this corresponds to reported work on the temperature dependency for phosphorus-based flame inhibition [34]. The effect of DMMP on the relative <sup>·</sup>OH concentration profiles was measured using quenching-corrected Laser-Induced Fluorescence (LIF) [35]. As the stoichiometric adiabatic flame temperature increased there was a strong decrease in the

magnitude of the reduction in  $\cdot\text{OH}$  concentration. Kinetic calculations show that inhibition is due to the phosphorus-containing radical  $\cdot\text{PO}_2$ , and  $\text{HOPO}$  and  $\text{HOPO}_2$ , formed after the decomposition of the parent compound; reactions involving phosphorus remove  $\text{H}\cdot$  and  $\cdot\text{O}\cdot$  atoms from the radical pool, thus weakening the flame. These reactions *produce*  $\cdot\text{OH}$  directly, and the  $\cdot\text{OH}$  concentrations are only indirectly reduced through reduction of  $\cdot\text{O}\cdot$  and  $\text{H}\cdot$  concentrations.

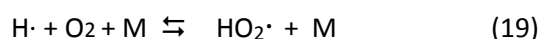
#### 4.5.1 Hydrogen cyanide formation and destruction in fires

The increased yield of  $\text{CO}$  in the current work follows directly from the inhibition of the free radical reactions by trapping active radicals such as  $\text{H}\cdot$  and  $\cdot\text{OH}$ . The increased yield of  $\text{HCN}$  by halogens, requires a clearer understanding of  $\text{HCN}$  formation and destruction in flames.

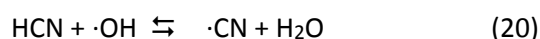
$\text{HCN}$  is a flammable gas with a lower explosive (ignitability) limit of 5.6% in air. In atmospheric science, biomass burning is the main source of atmospheric  $\text{HCN}$  [36]; similar to  $\text{CO}$ , it is removed from the atmosphere by reaction with the hydroxyl ( $\cdot\text{OH}$ ) radical. Combustion of nitrogenous materials releases nitrogen as  $\text{HCN}$  and ammonia ( $\text{NH}_3$ ), producing nitrous oxide ( $\text{N}_2\text{O}$ ) and nitric oxide ( $\cdot\text{NO}$ ). As the ratio of oxygen to nitrogen in the fuel increases, so the  $\text{HCN}/\text{NH}_3$  and  $\text{N}_2\text{O}/\text{NO}$  ratios decrease. Higher equivalence ratios and heating rates, and temperatures above  $727^\circ\text{C}$  favour  $\text{HCN}$  formation [36]

Reports of a novel study [37, 38] on  $\text{HCN}$  generation from combustion of polyamide 6.6 in the steady state tube furnace provide additional insight into the processes of  $\text{HCN}$  formation and destruction. In these experiments, infrared polarisation spectroscopy was used to measure the concentration of  $\text{HCN}$  inside the furnace tube, both close to the flame, and in the cool zone towards the exit of the furnace tube. Different fire conditions were investigated. In each case, the highest  $\text{HCN}$  concentrations were observed above the flame zone, and these diminished significantly for low temperature, well-ventilated flaming, and also for under-ventilated flaming at high temperature, but diminished least for small under-ventilated flaming (Stage 3a in Table 1).

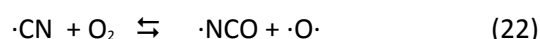
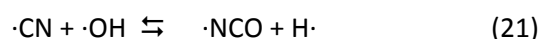
Currently accepted mechanisms, described in detail elsewhere, [36] indicate that  $\text{HCN}$  oxidises via a complex set of reactions, yielding  $\text{NO}$ ,  $\text{N}_2\text{O}$ ,  $\text{N}_2$ ,  $\text{CO}$ ,  $\text{CO}_2$  and water. A detailed scheme involving 41 species and 250 reversible reactions has been proposed [36] and validated through numerous experimental studies. Sensitivity analysis was used to identify the most important steps of mechanism. These include the hydrogen-oxygen chain branching steps, reactions 1, 2 (described earlier) and 19, a third-body recombination reaction.



Initially,  $\text{HCN}$  reacts with the  $\cdot\text{OH}$  radicals to form cyanide radicals ( $\cdot\text{CN}$ )

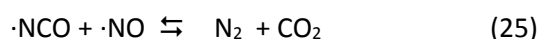
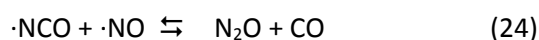
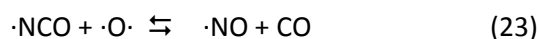


These are then oxidised to the isocyanate radical ( $\cdot\text{NCO}$ ) by  $\text{OH}\cdot$  and  $\text{O}_2$

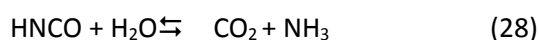




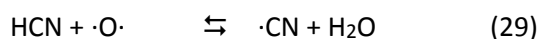
The isocyanate radical then combines with  $\cdot\text{O}\cdot$  to form  $\cdot\text{NO}$  and CO (23), or with nitric oxide to form  $\text{N}_2\text{O}$ ,  $\text{N}_2$ , CO and  $\text{CO}_2$  (24, 25).  $\cdot\text{NO}$  is a stable free radical which exists as a gas at room temperature.



HCN may also undergo reaction with  $\cdot\text{OH}$  to become cyanuric acid (HOCN) (26) which exists as a stable, non-toxic solid trimer, or isocyanuric acid (HNCO) (27) which readily hydrolyses (28).



Reactions 29 and 30 are also important, but only under fuel rich conditions [36].



This mechanism underlines the critical role played by the  $\cdot\text{OH}$  radical in the oxidation of HCN, particularly in well-ventilated conditions.

## 4.6 Effects of AlPiM and BrSb on toxic products yields of PA 6 and PA 6.6

The critical role played by the  $\text{OH}\cdot$  radical in reducing the concentration of CO and HCN, and hence the toxicity of fire effluents has been demonstrated. In addition to its unique role in oxidising CO to  $\text{CO}_2$  (reaction 10), it is also essential to the effective destruction of HCN (reactions 20, 26 and 27 in the current work). This has been demonstrated experimentally in the steady-state tube furnace in well-ventilated fires involving polyamides. The higher yields of both HCN and CO seen in well-ventilated flames of polyamides protected with brominated flame retardants and an antimony oxide synergist, presumably result from the removal of the  $\text{OH}\cdot$  radical from the flame zone. Moreover, the lower yields from PA formulations fire retarded by aluminium phosphinate/melamine polyphosphate combinations especially at higher temperatures, is a direct consequence of the different flame retardant mechanism of phosphorus, which only indirectly reduces the  $\cdot\text{OH}$  concentration, and achieves its flame quenching effects from reducing the  $\text{H}\cdot$  and  $\cdot\text{O}\cdot$  concentrations. Thus, this new generation of gas phase flame retardants, based on AlPi and MPP, not only reduce the ignitability and flame spread, they do so without a significant detrimental impact on the fire toxicity.

## 5 Conclusions

Although the overall number of casualties from fires have decreased, deaths and injuries from inhalation of toxic fire effluents, as a proportion of total fire victims, has continuously increased since the 1960s, for example, as reported in the UK fire statistics [1]. It has already been established and reported that carbon monoxide yields are increased by gas phase flame retardants, and by under-ventilation. Moreover, it has been shown that hydrogen cyanide yields also increase as fires become under-ventilated.

This work clearly shows that HCN is the major contributor to the toxicity for all fire retarded PA materials reported here, even in well-ventilated conditions, although the contribution from CO from the BrSb materials is also significant. This work shows that when comparing two formulations of comparable flammability, the one with the flame retardant containing bromine and antimony causes a significant increase in the fire toxicity, compared to the material flame retarded by the aluminium phosphinate/melamine polyphosphate blend. It demonstrates, for the first time, how hydrogen cyanide yields from aliphatic polyamides increase tenfold in the presence of a brominated flame retardant and antimony oxide, but only modestly, around twofold, in the presence of ALPiM. This has clear implications for fire safety: a fire of a 1 kg PA 6 fuse box flame retarded with the BrSb combination would produce a lethal effluent in a 10 m x 10 m x 3 m enclosure, where the same fuse box fire retarded with ALPiM would only produce a lethal volume of effluent for a 4.5 m x 5 m x 3 m enclosure. Thus while both fire retardant combinations reduce the risk of fire, if a fire does occur, the use of BrSb increases the hazard by increasing the fire toxicity much more than the ALPiM. Unfortunately, the development of brominated polystyrene to replace the current generation of brominated flame retardants has been shown to significantly increase the fire hazard. It also shows a positive correlation between furnace temperature and toxicity for the BrSb system, but a strongly negative correlation for ALPiM with furnace temperature, for both PA 6 and PA 6.6.

Bringing studies of flame retardant mechanisms together with gas phase kinetics of HCN formation and destruction has provided a crucial insight into the cause of this behaviour, through the differences in the gas phase inhibition mechanisms of the BrSb and ALPiM systems. In particular, the preferential trapping of the H· and ·O· radicals by ALPiM, leaving the ·OH radicals to oxidise the HCN and CO explains the significant reduction in fire effluent toxicity. The temperature effect of the phosphorus flame retardant systems provides crucial supporting evidence.

This study comes at a time when there is considerable pressure to eliminate all brominated flame retardants from consumer-products and replace them with safer alternatives. It presents experimental data, together with a detailed explanation which shows a significant fire safety advantages to replacing brominated flame retardants with aluminium phosphinate/melamine polyphosphate combinations. Brominated flame retardants have been shown to increase the yields of the two biggest killers in fires (CO and HCN), where their phosphinate replacements actually show a reduction in the fire toxicity, most notably as the fire grows and the temperature increases.

### *Acknowledgements*

This work was followed from the European project STREP FP-6 PredFire-Nano 'Predicting Fire Behaviour of Nanocomposites from Intrinsic Properties' under the contract STREP 013998, with

technical and financial support from Clariant Produkte (Deutschland) GmbH, a member of the PREDFIRE consortium. One of us (SAM) would like to thank the University of Central Lancashire for provision of PhD studentship.

- 
- 1 Fire Statistics United Kingdom 2008, Department for Communities and Local Government, London, 2010 (and preceding editions).
  - 2 Stec AA, Hull TR (Editors), Fire Toxicity, Woodhead Publishing, Cambridge, UK and CRC Press, Boca Raton, 2010.
  - 3 Stec AA, Hull TR, Lebek K, Purser JA, Purser DA. The effect of temperature and ventilation condition on the toxic product yields from burning polymers. *Fire Mater* 2008;32:49-60.
  - 4 Alarie Y. Toxicity of fire smoke. *Crit Rev Toxicol* 2002;32:259-89.
  - 5 Purser D. Toxicity of fire retardants in relation to life safety and environmental hazards, in *Fire retardant materials*, Edited by A R Horrocks and D Price, Woodhead publishing, Cambridge, UK 2001.
  - 6 Braun E, Gann R G, Levin B C, and Paabo M, Combustion Product Toxic Potency Measurements: Comparison of a Small Scale Test and "Real-World" Fires, *Journal of Fire Sciences* 1990 8: 63-79
  - 7 ISO 19706:2007 Guidelines for assessing the fire threat to people
  - 8 Pitts WM. The global equivalence ratio concept and the formation mechanisms of carbon monoxide in enclosure fires. *Progress in Energy and Combustion Science* 1995;21:197-237
  - 9 Hull TR, Paul KT, Bench-scale assessment of combustion toxicity - A critical analysis of current protocols, *Fire Safety Journal*, 2007; 42: 340-365.
  - 10 ISO TS 19700:2007 Controlled equivalence ratio method for the determination of hazardous components of fire effluents
  - 11 Stec AA, Hull TR, Lebek K. Characterisation of the steady state tube furnace (ISO TS 19700) for fire toxicity assessment. *Polym Degrad Stab* 2008;93:2058-65.
  - 12 ISO 13344:2004 Estimation of the lethal toxic potency of fire effluents
  - 13 ISO 13571:2012 Life threat from fires – Guidance on the estimation of time available for escape using fire data.
  - 14 Hull TR, Stec AA, Lebek K, Price D. Factors affecting the combustion toxicity of polymeric materials. *Polym Degrad Stab* 2007;92:2239-46.
  - 15 Stec AA, Hull TR. Assessment of the fire toxicity of building insulation materials. *Energy Build* 2011;43:498-506.
  - 16 Braun U, Schartel B, Fichera MA, Jäger C. Flame retardancy mechanisms of aluminium phosphinate in combination with melamine polyphosphate and zinc borate in glass-fibre reinforced polyamide 6,6. *Polym Degrad Stab* 2007;92:1528-45.
  - 17 Levchik, S. V., and Weil, E. D., A Review of Recent Progress in Phosphorus-based Flame Retardants, *Journal of Fire Sciences*, 24, 345, (2006)
  - 18 de Wit CA. An overview of brominated flame retardants in the environment, *Chemosphere*, 46, 583, (2002).
  - 19 Shaw SD, Blum A, Weber R, Kannan K, Rich D, Lucas D, Koshland CP, Dobraca D, Hanson S, Birnbaum LS. Halogenated flame retardants: Do the fire safety benefits justify the risks? *Rev Environ Health* 2010;25:261-305.
  - 20 Birnbaum LS, Staskal DF. Brominated flame retardants: Cause for concern? *Environ Health Perspect* 2004;112:9-17.
  - 21 J DiGangi, A Blum, Å Bergman, C. A. de Wit, D Lucas, D Mortimer, A Schechter, M Scheringer, S D. Shaw and T. F. Webster San Antonio Statement on Brominated and Chlorinated Flame Retardants, *Environmental Health Perspectives*, **118**, A 516-536, 2010.
  - 22 Newton PE; Schroeder RE; Zwick L; Serex T; Inhalation Developmental Toxicity Studies In Rats With Antimony Trioxide (Sb2O3). *Toxicologist* 2004 Mar;78(1-S):38

- 
- 23 Hull TR, Carman JM, Purser DA. Prediction of CO evolution from small-scale polymer fires. *Polym Int* 2000;49:1259-65.
  - 24 A Schnipper, L Smith-Hansen, S E Thomsen, Reduced Combustion Efficiency of Chlorinated Compounds, Resulting In Higher Yields of Carbon Monoxide, *Fire and Materials*, **19**, 61-64, (1995).
  - 25 Babushok, V. Tsang, W., Linteris, G. T., and Reinelt, D. (1998) Chemical Limits to Flame Inhibition, *Combustion and Flame*, 115:551-560.
  - 26 Linteris GT, Rumminger MD, Babushok VI. Catalytic inhibition of laminar flames by transition metal compounds. *Progress in Energy and Combustion Science* 2008;34:288-329.
  - 27 Samyn F, Bourbigot S. Thermal decomposition of flame retarded formulations PA6/aluminum phosphinate/melamine polyphosphate/organomodified clay: Interactions between the constituents? *Polym Degrad Stab* 2012;97:2217-30.
  - 28 Werner JH, Cool TA. Kinetic model for the decomposition of DMMP in a hydrogen/oxygen flame. *Combust Flame*. 1999;117:78-98.
  - 29 Kan W, Zhong H, Yu H. Theoretical prediction regarding structural and thermodynamical characteristics of stable CH<sub>3</sub>PO<sub>2</sub> isomers and unimolecular decomposition mechanisms of species CH<sub>3</sub>P(=O)<sub>2</sub>, CH<sub>3</sub>O-P=O, and CH<sub>2</sub>=P(=O)OH. *Journal of Computational Chemistry*. 2009;30:2334-2350.
  - 30 Brinkmann, N. R., and Carmichael, I., B3LYP Investigation of HPO<sub>2</sub>, trans-HOPO, cis-HOPO, and Their Radical Anions, *J. Phys. Chem. A*, 108, 9390-9399, (2004).
  - 31 Babushok, V., and Tsang, W., Influence of Phosphorus-Containing Fire Suppressants on Flame Propagation, *Proc. Third Int. Conf. on Fire Res. and Eng.*, Chicago, IL, p. 257-267 (1999).
  - 32 Kaczorek, K.; Stec, A. A.; Hull, T. R. *Carbon monoxide generation in fires: Effect of temperature on halogenated and aromatic fuels*; *Fire Safety Science*; 2011; 10, 253-263.
  - 33 Kaczorek K, Stec AA, Hull TR. Carbon monoxide generation in fires: Effect of temperature on halogenated and aromatic fuels. *Fire Safety Science*. 2011:253-263
  - 34 Hastie, J. W. and Bonnell, D. W., *Molecular Chemistry of Inhibited Combustion Systems*, National Bureau of Standards, Final NBSIR 80-2169 ; PB81-170375, (1980).
  - 35 M.A. MacDonald, F.C. Gouldin and E.M. Fisher, Temperature dependence of phosphorus-based flame inhibition, *Combustion and Flame*, 124, 668-683, (2001).
  - 36 Dagaut, P., Glarborg, P., Alzueta, M. U., The oxidation of hydrogen cyanide and related chemistry, *Progress in Energy and Combustion Science* 2008; 34: 1-46.
  - 37 Sun ZW, Försth M, Li ZS, Li B, Aldén M. Mid-infrared polarization spectroscopy: A tool for in situ measurements of toxic gases in smoke-laden environments, *Fire and Mater*, 2011; 35: 527-537.
  - 38 Sun Z, Försth M, Li Z, Li B, Aldén M, In situ Measurements of HCN in a Tube Furnace with Infrared Polarization Spectroscopy, *Fire Safety Sci*, 2011; 10.